Liposomal sunitinib for ocular drug delivery : A potential treatment for choroidal neovascularization

Tavakoli, Shirin

2022-05-25

Tavakoli , S , Puranen , J , Bahrpeyma , S , Lautala , V E , Karumo , S , Lajunen , T , del Amo , E M , Ruponen , M & Urtti , A 2022 , ' Liposomal sunitinib for ocular drug delivery : A potential treatment for choroidal neovascularization ' , International Journal of Pharmaceutics , vol. 620 , 121725 . https://doi.org/10.1016/j.ijpharm.2022.121725

http://hdl.handle.net/10138/347477
https://doi.org/10.1016/j.ijpharm.2022.121725

International Journal of Pharmaceutics 620 (2022) 121725

Contents lists available at ScienceDirect

International Journal of Pharmaceutics

journal homepage: www.elsevier.com/locate/ijpharm

Liposomal sunitinib for ocular drug delivery: A potential treatment for choroidal neovascularization

Shirin Tavakoli [a], Jooseppi Puranen [b], Sina Bahrpeyma [b], Veera E. Lautala [a], Suvi Karumo [a], Tatu Lajunen [a,b,c], Eva M. del Amo [b], Marika Ruponen [b], Arto Urtti [a,b,*]

[a] Drug Research Program, Division of Pharmaceutical Biosciences, Faculty of Pharmacy, University of Helsinki, Viikinkaari 5 E, FI-00790 University of Helsinki, Finland
[b] School of Pharmacy, Faculty of Health Sciences, University of Eastern Finland, Yliopistonranta 1, 70210 Kuopio, Finland
[c] Laboratory of Pharmaceutical Technology, Department of Pharmaceutical Science, Tokyo University of Pharmacy & Life Sciences, 1432-1 Hachioji 192-0392, Tokyo, Japan

ARTICLE INFO

Keywords:
Liposome
Sunitinib
Choroidal neovascularization
Age-related macular degeneration
Cyclodextrin
Intravitreal injection

ABSTRACT

Choroidal neovascularization (CNV) is a prevalent vision-threatening vascular disorder in aging population. CNV is associated with several diseases in the posterior segment of the eye such as age-related macular degeneration (AMD). In this study we developed sunitinib-loaded liposomes to block the neovascularization signalling pathway through inhibition of tyrosine kinase of vascular endothelial growth factor receptors (VEGFRs). Liposomal sunitinib formulations were prepared by thin film hydration method and studied for their encapsulation efficiency (EE), loading capacity (LC) and drug release profile in buffer andvitreous. Our finding showed that the liposomes (mean size 104 nm) could effectively entrap sunitinib (EE ≈ 95%) at relatively high loading capacity (LC ≈ 5%) and release sunitinib over at least 3 days. Intravitreal sunitinib-loaded liposomes revealed inhibitory effect on established neovascularization in laser-induced CNV mouse model while the intravitreal injection of sunitinib solubilized with cyclodextrin was inefficient in management of neovascularization. Accordingly, liposomal sunitinib is a promising drug delivery system that should be further studied to inhibit the CNV related to AMD.

1. Introduction

Ocular pathological neovascularization is the most common cause of vision loss in industrialized countries (Campochiaro, 2013; Ferrara, 2016). In choroidal neovascularization (CNV) newly formed blood vessels sprout from choriocapillaries and grow into the subretinal space through Bruch's membrane and RPE (Campochiaro, 2013). Choroidal neovascularization is a hallmark of exudative age-related macular degeneration (AMD), also known as wet-AMD; a prevalent vision-threatening ocular disease (Jager et al., 2008). The number of AMD patients increase worldwide at fast rate. The number of patients has been projected to reach over 240 million cases worldwide between 2020 and 2030 (1.2-fold increase) (World report on vision, 2020) (Wong et al., 2014). The AMD affects the quality of life of increasing number of individuals socially and economically.

The current AMD therapy includes intravitreal injections of vascular endothelial growth factor (VEGF) neutralizing agents, such as ranibizumab, bevacizumab, aflibercept and brolucizumab (Varela-Fernández et al., 2020; Ferrara and Adamis, 2016; Al-Khersan et al., 2019). The VEGF inhibitors transformed the treatment of wet-AMD that was earlier based on phototherapy by verteporfin (Visudyne®) (Ferrara and Adamis, 2016; Patel et al., 2018). The current treatment prevents the interaction between VEGF and its receptor (mainly VEGFR-2), since binding to VEGFR-2 triggers the endothelial cell migration and proliferation (Ferrara, 2016; Ferrara and Adamis, 2016). The VEGF inhibitors are delivered as monthly or bimonthly intravitreal injections to millions of patients (Janoria et al., 2007; Peyman et al., 2009). Despite their significant therapeutical benefits, current anti-VEGF drugs show unsatisfactory therapeutic response even in more than 20% of the patients due to various reasons (Sakurai et al., 2005). There is still a need for additional therapeutics in the treatment of neovascular AMD.

It is now evident that the phosphorylation of tyrosine in VEGFRs is required for the neovascularization signalling pathway (Sakurai et al., 2005). Thus, an alternative strategy is to block the VEGF-induced signalling pathway by tyrosine kinase inhibitors (e.g. sunitinib, axitinib and pazopanib) (Al-Khersan et al., 2019; Robbie et al., 2013; Nowak-

* Corresponding author.
E-mail address: arto.urtti@helsinki.fi (A. Urtti).

https://doi.org/10.1016/j.ijpharm.2022.121725
Received 24 January 2022; Received in revised form 1 April 2022; Accepted 5 April 2022
Available online 8 April 2022

Sliwinska et al., 2015; Giddabasappa et al., 2016). Sunitinib received FDA approval for treatment of renal cell carcinoma (Motzer et al., 2006) and has shown effective suppression of VEGF expression in several *in vitro* and *in vivo* studies with ARPE19 cell line (Streets et al., 2020), chick embryo chorioallantoic membrane (CAM) (Ramazani et al., 2015) and animal models (mouse, rat, rabbit) (Tsujinaka et al., 2020). Sunitinib has broad mechanism of action by blocking all VEGFRs (VEGFR1-VEGFR3) and platelet-derived growth factor (PDGFR) that are associated with neovascularization (Roskoski, 2007). Hence, it may provide better visual outcomes than the current anti-VEGF treatments.

Given the dose-dependent toxicity and small molecular size of sunitinib, intravitreal administration is only practical by using drug delivery systems (del Amo et al., 2017). Dissolved sunitinib is eliminated from the vitreous cavity rapidly (half-life in rabbit eye is 3.7 h) due to its ability to cross blood-retinal barrier (Del Amo et al., 2015). In this study, we developed a liposomal sunitinib formulation according to our previously reported criteria for the design of intravitreal nanocarriers (Tavakoli et al., 2021; Tavakoli et al., 2020). Sunitinib-loaded liposomes were applied to 1) suppress the VEGF-induced neovascularization and 2) extend the drug release in the vitreous. We examined the physicochemical formulation features and anti-neovascularization effects of liposomal sunitinib in laser-induced CNV mice model.

2. Materials and methods

2.1. Materials

1,2-distearoyl-*sn*-glycero-3-phosphocholine (DSPC), 1,2-dioleoyl-*sn*-glycero-3-phosphocholine (DOPC), 1,2-distearoyl-*sn*-glycero-3-phosphoethanolamine-N-[amino(polyethylene glycol)-2000] (DSPE-PEG) and 1,2-distearoyl-*sn*-glycero-3-phosphoglycerol (DSPG), were purchased from Avanti Polar Lipids, Inc. (Alabaster, AL, USA). The extruder was purchased from Avanti Polar Lipids (Alabaster, AL, USA) and the 100 nm Nucleopore polycarbonate membranes (diameter 19 mm) were supplied from Whatman Int. Ltd. (Maidstone, England). Frozen citrate–phosphate-dextrose (CPD)-anticoagulated human plasma was bought from the Finnish Red Cross Blood Service (Helsinki, Finland), which is provided as an anonymized blood product for research use only and constitutes non-identifiable human material under the Declaration of Helsinki. Vitreous humour for drug release experiments was isolated from porcine eyes provided by HKScan Finland Oy (Forssa, Finland) and homogenized according to the protocol reported previously (Jager et al., 2008) (World report on vision, 2020). Amicon ® Ultra-4, MWCO 10 kDa was supplied by Merck-Millipore®, USA. Sunitinib free base (S-8877) was purchased from LC Laboratories (Woburn, MA, USA). Slide-A-Lyzer® mini dialysis device with 10 K MWCO inserts was supplied by Thermo Fisher Scientific. Triton X-100 was from MP Biomedicals (Santa Ana, CA, USA). Dulbecco's phosphate buffer saline (PBS) was supplied from Gibco®. 4-(2-hydroxyethyl)-1-piperazineethanesulfonic acid (HEPES), sodium chloride (NaCl), Hydroxypropyl β-cyclodextrin and all organic solvents were purchased from Sigma-Aldrich (St. Louis, MO, USA). All reagents were analytical grade.

2.2. Sunitinib analysis by ultra-performance liquid chromatography (UPLC)

Sunitinib quantification was performed using the Acquity UPLC (Waters, USA). Briefly, a gradient method was applied with a mobile phase A (0.015 M phosphate buffer, pH 2) and mobile phase B (acetonitrile) using a Luna Omega 1.6 μm Polar C18 column (100 Å, 2.1 mm × 50 mm, Phenomenex, USA) at a flow rate of 0.5 ml/min. The eluent ratio (A/B) was linearly changed from 70/30 to 40/60 in 2 min after which the system was stabilized for 1 min. The detection wavelength of sunitinib was 270 nm. The volume of injection was 5 μL and the running time for all samples was 3 min. The retention time of sunitinib was 0.85 min.

2.3. Sunitinib-cyclodextrin inclusion complexes: phase solubility assay

Solubility test was performed according to the phase solubility assay as described by Higuchi and Connors (Higuchi and Connors, 1965). A known excess amount of sunitinib was added to various concentrations of hydroxypropyl β-cyclodextrins (1, 2.5, 5, 10, 20, 40, 60, 80, 120, 160 mM) in 1.5 ml of PBS. The suspensions were shaken at the speed of 300 rpm for 48 h at 25° C. The samples were then filtered through a 0.45 μm polytetrafluoroethylene (PTFE) filter and assayed for dissolved sunitinib content by UPLC.

2.4. Liposome preparation

Liposomes were prepared by thin film hydration method followed by sequential extrusion as reported previously with a modification in the lipid composition (Kari et al., 2020). DSPC, DOPC, DSPG and DSPE-PEG lipid mixture (20 μmol) at a molar ratio of 75:10:10:5, respectively, were dissolved in chloroform and placed in rotary evaporator. In order to form a thin lipid layer, the organic solvent was removed at 55 °C under nitrogen flow while the pressure was gently reduced to below 100 mbar. The thin lipid film was then hydrated with 1 ml of HEPES buffer saline solution (20 mM HEPES and 140 mM sodium chloride, pH 7.4) at the indicated temperature. Thereafter, liposomes were extruded 11 times at 55 °C through polycarbonate filter membranes of 100 nm pore size with a syringe-type mini-extruder (Avanti Polar Lipids) followed by quick cooling and storing at 4 °C. Given the highly lipophilic characteristic of sunitinib (LogP = 2.93), encapsulation of sunitinib was done by adding the sunitinib (7% w/w to lipids in chloroform) to the lipid mixture in chloroform prior to evaporation process.

2.5. Sunitinib-liposome characterization

2.5.1. Size and zeta potential

The particle size was measured by dynamic light scattering (DLS) using Malvern Zetasizer APS automated plate sampler (Malvern Instruments Ltd., Malvern, United Kingdom). Data acquisition was performed with Malvern DTS v7.01 software and the result were reported as size distribution by particle number and polydispersity index (PdI). Prior to measurement, each sample was diluted at 1:10 v/v ratio in HEPES buffer (pH 7.4) and analyzed three times with 13 sub-runs. The zeta potential was determined following the same sample dilution at room temperature with a Zetasizer ZS v7.1.1 (Malvern Instruments Ltd.).

2.5.2. Encapsulation efficiency and loading capacity

Encapsulation efficiency was calculated by indirectly determining the amount of drug entrapped in the liposomes and defined as the percentage of drug incorporated into liposomes relative the total amount of drug used in the preparation (Eq. (1)). Loading capacity was calculated to determine the amount of encapsulated sunitinib relative to the amount of liposomes in the formulation (Eq. (2)). Since sunitinib has poor solubility, solid sunitinib was first separated from dissolved and liposomal sunitinib by centrifuging at 12,800*g* for 10 min (Thermo IEC microlite microcentrifuge, USA). Then, the supernatant was collected in Polyaallomer tube (Beckman Coulter®, USA) and ultracentrifuged at 215,000*g* for 2 h using a SW 60 Ti rotor in ultracentrifuge (Optima Max, Beckmann Coulter, USA) at 20 °C. The clear supernatant contains the free dissolved sunitinib, whereas the sunitinib loaded liposomes formed a gel-like pellet. The components were kept at 4 °C until analysis.

The encapsulation efficiency (EE%) and loading capacity (LC%) were calculated by following equations:

$$\text{Encapsulation efficiency (EE\%)} = \frac{A_{\text{total drug}} - A_{\text{free drug}}}{A_{\text{total drug}}} \times 100, \quad (1)$$

$$\text{Loading capacity (LC\%)} = \frac{A_{\text{total drug}} - A_{\text{free drug}}}{A_{\text{total liposome}}} \times 100, \quad (2)$$

where $A_{total\ drug}$ is the total amount of the sunitinib used in the formulation and $A_{total\ liposome}$ in Eq. (2) is the total amount of lipids.

2.6. In vitro drug release

Slide-A-Lyzer® mini dialysis device with 10 K MWCO inserts was used for drug release study. The donor compartment volume holds a fixed volume of 500 μL and the receiver compartment volume is 14 ml. The receiver compartment was filled with DPBS (pH 7.4) with excess amount of HP β-CD (15 mM) to maintain the sink conditions. The liposomal sunitinib formulation was first purified with Amicon ® Ultra-4, MWCO 10 kDa spin filter at 12,000*g* for 15 min. Next, the formulations were mixed (1:1 v/v) with two different media: 1) DBPS buffer and 2) premixed porcine vitreous and placed in the donor compartment. All donor chambers were supplemented with 1% cell culture grade penicillin–streptomycin. The dialysis devices were placed in orbital shaker and kept at +37 °C under shaking at 300 rpm in an incubator. At certain time points, 100 μL of sample was withdrawn from each receiver compartment and the equivalent volumes of DPBS containing HP β-CD was replaced in the receiver chamber. The samples were mixed with phosphate buffer (pH = 2) at 1:2 or 1:5 v/v ratio. Then 5 μL of the sample was withdrawn and analyzed using UPLC method. Sunitinib- HP β-CD complexes were studied in similar experimental set-up as a control for the dialysis membrane barrier.

The cumulative release of sunitinib (%) was calculated according to Eq. (3) as follows:

$$\text{Amount in the dialysis device, } A_t = [C_t \times V_t]$$

$$\text{Removed amount from dialysis device, } R_t = [C_t \times V_s]$$

$$\text{Cumulative release } (\%)\frac{M_t}{M_\infty} = \frac{\sum_0^{t-1} Rt + A_t}{\text{Total amount}} \times 100 \quad (3)$$

where M_t/M_∞ is the fraction of compound released at a time t and C_t is sample concentration (μM). Total dialysis device volume and sample volume were shown as V_t and V_s (L), respectively. Total amount is the initial measured drug per device (μmol).

Sunitinib-cyclodextrin complex stability was assessed in separate vials while protecting from light at 4 °C and 37 °C over the course of study and the sunitinib concentration was analyzed by UPLC (see Section 2.2).

2.7. In vivo anti-neovascularization studies

2.7.1. Animal model for choroidal neovascularization

Male C57Bl/6JRccHsd mice, eight weeks old, from Envico Laboratories (UK) were used. The mice were housed in a controlled environment (temperature 21 ± 1 °C, 12-h light/dark cycle) with standard diet and water ad libitum. All experiments were designed and conducted according to the guidelines of the ARVO Statement for the Use of Animals in Ophthalmic and Vision Research and they were approved by the Finnish National Animal Experiment Board (ESAVI-2020-027769).

Before inducing CNV, the mice were anesthetized with intraperitoneal injection of 50 mg/kg ketamine (Ketaminol®; Intervet International B.V. Boxmeer, Netherland) and 1 mg/kg (Domitor®; Orion Oy, Tampere, Finland) medetomidine and pupils were dilated with topical application of 0.5% tropicamide (Oftan® Tropicamid, Santen Pharmaceuticals Co, Ltd.,Tampere, Finland). CNV was induced to all animals by retinal photocoagulation laser (Vitra 2; Quantal Medical, Rockwall, TX, USA). Four laser spots were placed around the optic disc of both eyes (power 100 mW; exposure 100 ms; spot size 50 μm). The bubble formation indicated the induction of CNV through a rupture of Bruch's membrane. Lesions with hemorrhage were excluded from further studies.

The formation and development of CNV were monitored using optical coherence tomography (OCT) and fluorescein fundus angiography (FA) using Micron IV instrument (Phoenix Research Labs, Pleasanton, CA, USA). OCT and FA images were obtained on days 0, 3 and 7. Angiograms at five-minute phase were used for comparative analyses. The area of leakage was outlined and calculated as the number of pixels in a masked fashion by ImageJ software (National Institute of Health, Bethesda, MD, USA). Each treatment group (liposomal sunitinib, sunitinib-cyclodextrin or aflibercept) was compared to the control group using two-tailed unpaired *t*-test with unequal variance. All results were expressed as mean ± SD. Differences were considered statistically significant at $p < 0.05$.

2.7.2. Intravitreal drug treatments

Two different experiment arms were used to evaluate the effects of liposomal sunitinib and sunitinib-cyclodextrin. In the first study on liposomal sunitinib, the mice were randomly divided into three groups immediately after laser photocoagulation. Under a deep plane of anesthesia 1 μL of drug formulation was injected intravitreally into both eyes using Hamilton microinjector (Hamilton Co., Reno, NV, USA). Group 1 (n = 10) received injection of aflibercept (Eylea® 40 mg/ml), group 2 (n = 10) received injection of sunitinib encapsulated in liposomes and group 3 (n = 10) received no treatment and acted as a control in this study.

In the second study a total of 12 mice were divided into two groups. All animals underwent laser photocoagulation as described above. Group 1 (n = 6) received 1 μL of sunitinib-cyclodextrin into both eyes (total dose, 5 μg of sunitinib). The mice of group 2 (n = 6) were used as controls. Topical eye drop (Viscotears®, Alcon, Finland) was applied after intravitreal injections to prevent any efflux of drugs.

3. Results

3.1. Physicochemical characterization of liposomes

The following physicochemical characteristics were measured for sunitinib-loaded liposomes: hydrodynamic diameter was 104 ± 28 nm, polydispersity index (PdI) 0.177, and ζ –potential −21.4 mV (Fig. S1). The formulations showed narrow size distribution as the PdI values were below 0.2.

3.2. Sunitinib-cyclodextrin inclusion

Fig. 1 demonstrates the phase solubility diagram applied for the complexation of sunitinib with HP β-CD. According to this diagram the solubility of sunitinib linearly elevates with increasing concentration of cyclodextrin. This confirms the "AL type" phase solubility diagram. The complexation of HP β-CD with sunitinib increased the solubility of

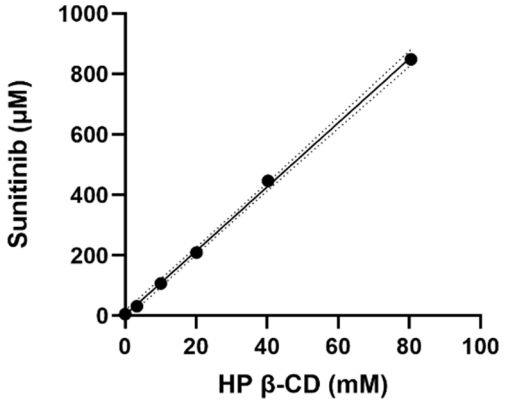

Fig. 1. Phase solubility diagram of sunitinib complexed with HP β-CD at various concentrations in DPBS at pH 7.4. Linear regression analysis was done in GraphPad Prism v.8 with 95% confidence interval, $r^2 = 0.9988$.

sunitinib by almost 150-fold, from 5.6 μM (without complexation) up to 848 μM at 80.4 mM of HP β-CD (Fig. 1). Accordingly, 15 mM of HP β-CD was selected for obtaining the sink conditions in the release study which is at least 5 times higher than the solubility of inserted dose.

3.3. Encapsulation efficiency and loading capacity of sunitinib in the liposomes

Sunitinib was passively loaded in liposomes using thin layer hydration technique. The encapsulation efficiency which represents the mass ratio of loaded drug to total drug in the system was 94.7 ± 11.0 % with relatively high loading capacity of 4.8% (loaded drug amount/lipid mass).

3.4. In vitro drug release

Drug release profile of liposomal sunitinib (Fig. 2) demonstrates that the complete release from liposomes in buffer and vitreous were obtained by 72 h and there were not significant difference between the drug release in the vitreous compared to the DPBS buffer. Sunitinib in HP β-CD complexes (without liposome) was used as a control. After 4 h the concentration of the sunitinib reached equilibrium in both donor and receiver chamber, indicating that the dialysis membrane does not limiting the sunitinib transfer between chambers.

Neither changes in sunitinib concentration nor extra peaks in UPLC analysis were observed in the stability experiment with sunitinib-cyclodextrin complexes suggesting that sunitinib was stable during the experiments (Fig. 3).

3.5. Liposomal sunitinib reduces choroidal neovascularization lesions

To determine the effect of liposomal sunitinib on laser induced CNV, fundus fluorescein angiography was performed. Laser spots in control mice showed remarkable leakage of fluorescein on experimental days 3 and 7 (Fig. 4). Single intraocular administration of liposomal sunitinib suppressed leakage on day 3 post-photocoagulation. The fluorescein leakage was 50% lower in the liposomal sunitinib-treated group compared to the control mice (3520 ± 4048 pixels vs. 7040 ± 5412 pixels in controls). In contrast, mice treated with aflibercept decreased leakage 58% on day 3 (2972 ± 3012 pixels) and 72% on day 7 (1474 ± 2491 pixels). There was no statistically significant difference between the control and liposomal sunitinib-treated groups at 7 days.

Fundus image acquisition and fluorescence intensity analyses

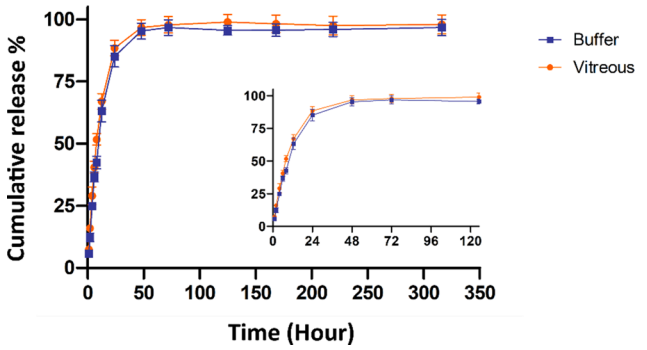

Fig. 2. The cumulative release of sunitinib (%) from liposomal formulation. Slide-A-Lyzer® mini dialysis device with 10 K MWCO inserts was used for drug release study. Donor compartment contained the liposomal sunitinib formulations which were mixed (1:1 v/v) with two different media: 1) DBPS buffer and 2) premixed porcine vitreous. The receiver chamber was filled with DPBS (pH 7.4) with excess amount of HP β-CD (15 mM) to maintain the sink conditions. The drug release study was performed in orbital shaker incubator at the speed of 300 rpm and + 37 °C. The insert shows a magnified view of release profile over 5 days. (n = 3).

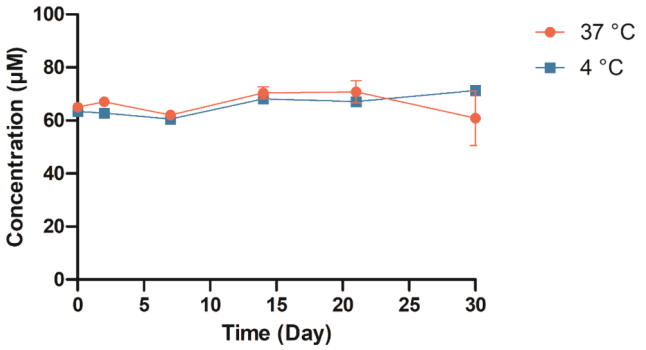

Fig. 3. Sunitinib stability at 37 °C and 4 °C during 30 days. (n = 3).

(Fig. S2) supports the conclusion that most sunitinib is eliminated in 3 days from the vitreous.

The analysis of the inhibitory effect of sunitinib-cyclodextrin on CNV fluorescein angiography was performed (Fig. 4). The fluorescein leakage did not differ significantly between the sunitinib-cyclodextrin and control groups on day 3 or day 7 (9619 ± 6589 pixels vs. 5911 ± 4578 pixels in controls; 6515 ± 6314 pixels vs. 7025 ± 8297 pixels in controls), respectively. In addition, our *in vivo* experiments did not show any sign of inflammation upon intravitreal injection of sunitinib-cyclodextrin complex based on OCT and fundus imaging.

4. Discussion

Sunitinib is a multiple tyrosine kinase inhibitor that blocks VEGF-induced neovascularization signalling through the VEGF and PDGF receptors (Ferrara and Adamis, 2016) (Robbie et al., 2013) (Roskoski, 2007). Thus, sunitinib may provide an alternative approach to anti-VEGF biologics in blocking VEGF-associated ocular neovascularization. Previously, Takahashi *et al,* reported inhibition of neovascularization in CNV mouse model following the oral administration of sunitinib (Takahashi et al., 2006), but this approach may not be feasible and safe in the clinics. Moreover, sunitinib revealed neuroprotective effect due to its inhibitory effect on dual-leucine zipper kinase (DLK) which may prevent retinal degenerative process in AMD as well as other ocular conditions with retinal degeneration including glaucoma (Welsbie et al., 2017) (Welsbie et al., 2019). Thus, sunitinib is an interesting compound for complementing the current therapeutic arsenal in the treatment of AMD, but problems of poor solubility and rapid intravitreal elimination of small molecules should be solved (del Amo et al., 2017; Del Amo et al., 2015; Schmitt et al., 2019).

Our approach combines a tyrosine kinase inhibitor sunitinib and liposome formulation to overcome its solubility problem and rapid clearance from the eye. Previously, we demonstrated that 100 nm sized PEGylated anionic liposomes are freely mobile in the vitreous with insignificant protein corona formation suggesting that they can overcome vitreal barrier (Tavakoli et al., 2021). In this study, we developed intravitreally injectable sunitinib liposomal formulation for retinal delivery to minimize drug dosing levels and risks of systemic sunitinib toxicity. We applied the sunitinib free base as a highly lipophilic form of the drug in order to maximize the encapsulation efficiency (about 95%) and loading capacity (≈5%), but sunitinib release studies were challenging due to its poor water-solubility. We solved the solubility issue by introducing excess of HP β-CD to the receiving chamber of dialysis device to maintain the sink condition. Sunitinib release from these liposomes took place in about 72 h. Considering the liposome structure and the high phase transition temperature, the liposomes were stable in the release condition, therefore the release mechanism is expected to be simple diffusion-controlled release (Jain and Jain, 2016).

A single intravitreal injection of liposomes with 1 μg of encapsulated sunitinib resulted in effective anti-neovascular effect for 3 days (Fig. 2),

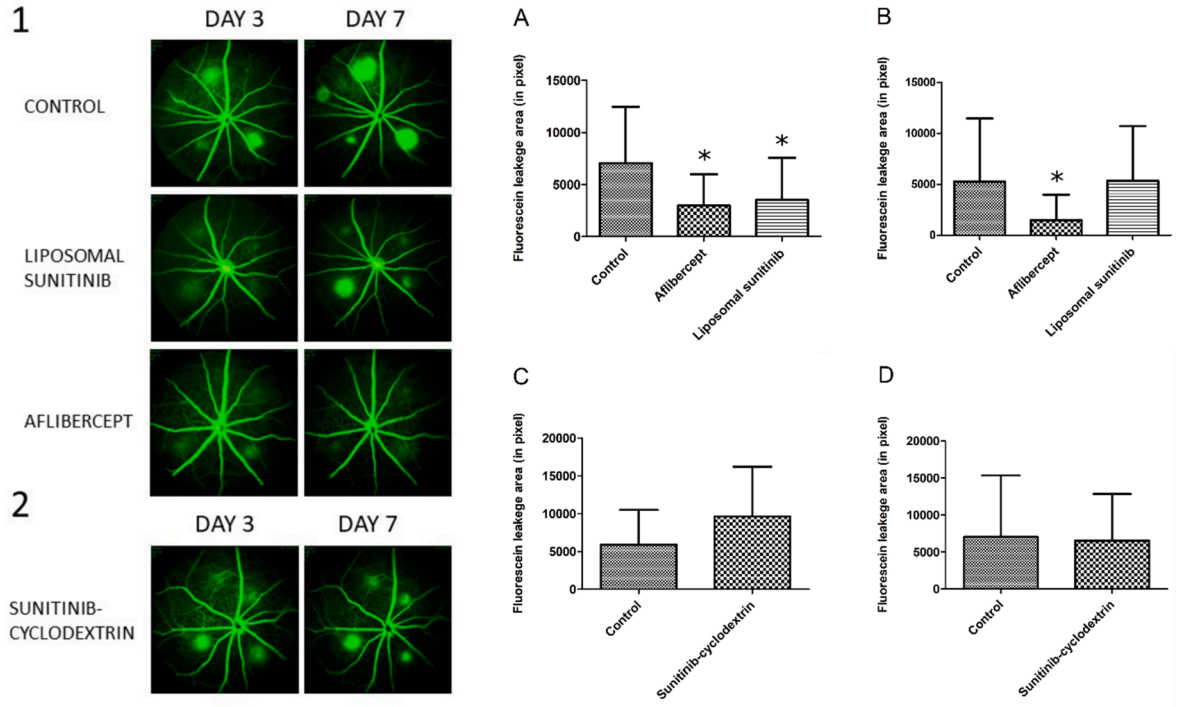

Fig. 4. *In vivo* analysis of the effect of 1. liposomal sunitinib (n = 20 eyes in control group; n = 20 eyes in aflibercept group; n = 20 eyes in liposomal sunitinib group) and 2. sunitinib-cyclodextrin (n = 12 eyes in control group; n = 12 eyes in sunitinib-cyclodextrin group) on vascular leakage. Representative late-phase fluorescein angiograms in control mice and in aflibercept, liposomal sunitinib and sunitinib-cyclodextrin treated mice, three days and seven days after photocoagulation are shown in the left side. Vascular leakage measured by fluorescein angiography as graphical illustrations: results of day 3 (1A and 2C) and day 7 (1B and 2D). Values are presented as mean ± SD. * denotes statistically significant difference compared to the controls ($p < 0.05$).

while the solution of sunitinib-HP β-CD complexes failed in preventing the vascular leakage (Fig. 4). This can be attributed to more rapid ocular elimination of the sunitinib-cyclodextrin complexes (estimated half-life ~4 h) (Schmitt et al., 2019) as compared to the liposomes as duration of sunitinib effect matched the elimination kinetics from the mouse eyes (Fig. S2) (del Amo et al., 2017) (Urtti, 2006). Thus, liposomes are better solubilization method than cyclodextrins for intravitreal sunitinib injections and the study also demonstrates that a delivery system is needed for utilization of sunitinib as an intravitreal injection. Previously, microparticles have been used to sustain sunitinib release and retention in the vitreous (Tsujinaka et al., 2020).

According to our fluorescein angiograms, liposomal sunitinib effectively prevents vascular leakage in CNV mice for 3 days, which is in agreement with *in vitro* drug release and liposome elimination from the mouse vitreous. As sunitinib-CD solution did not show any anti-neovascularization effect, the liposome effect kinetics can be attributed to drug release and reduced drug elimination from the vitreous humour. Even though vitreal retention and retinal actions of drugs are generally much longer in humans (vitreous volume 4 ml) than in mice (volume 5 μL) (Schmitt et al., 2019), we should note that liposomal sunitinib had shorter action than aflibercept in mouse eyes. Therefore, further optimization of sunitinib release and vitreal retention are needed to achieve at least monthly injection intervals in AMD treatment. On the other hand, permeation of liposomes to the retinal tissue and into the cells (Tavakoli et al., 2020) opens additional possibilities. For instance, sunitinib is a substrate for P-glycoprotein transporter in the RPE cells, and liposomal formulation might improve drug efficacy by bypassing the cellular efflux transport (Zhang et al., 2008).

Overall, nanosystems combine drug release in the vitreous with more localized delivery into the retina, even inside retinal cells (Roskoski, 2007), thus providing potential advantages in retinal drug delivery over microparticles and implants, but further research is needed to prolong drug release and liposomal retention in the vitreous and retina.

5. Conclusion

We have demonstrated that anionic PEG-coated liposomes effectively encapsulate the sunitinib and release the drug in the vitreous humour medium in 3 days. After intravitreal administration liposomal sunitinib reduced the vascular leakage in the CNV mouse model *in vivo* while solution formulation of sunitinib was ineffective. In summary, we have shown that liposomal drug delivery system may provide an efficient means for sunitinib delivery to the posterior segment of the CNV mouse eye suggesting possibilities for further development of retinal therapeutics.

CRediT authorship contribution statement

Shirin Tavakoli: Conceptualization, Methodology, Validation, Formal analysis, Investigation, Writing – original draft, Writing – review & editing, Visualization, Funding acquisition. **Jooseppi Puranen:** Conceptualization, Methodology, Validation, Formal analysis, Investigation, Writing – original draft, Writing – review & editing, Visualization. **Sina Bahrpeyma:** Methodology, Validation, Formal analysis, Investigation, Writing – review & editing, Funding acquisition. **Veera E. Lautala:** Investigation. **Suvi Karumo:** Investigation. **Tatu Lajunen:** Methodology, Writing – review & editing, Supervision, Resources, Project administration, Funding acquisition. **Eva M. del Amo:** Writing – review & editing, Supervision. **Marika Ruponen:** Methodology, Writing – review & editing, Supervision, Resources, Project administration. **Arto Urtti:** Conceptualization, Resources, Writing – review & editing, Supervision, Project administration, Funding acquisition.

Declaration of Competing Interest

The authors declare the following financial interests/personal relationships which may be considered as potential competing interests:

Arto Urtti reports financial support was provided by Business Finland. Arto Urtti reports financial support was provided by Horizon 2020. Tatu Lajunen reports financial support was provided by Phospholipid Research Center. Tatu Lajunen reports financial support was provided by Instrumentarium Science Foundation. Tatu Lajunen reports financial support was provided by Silmäsäätiöiden Tohtoritutkijapooli. Eva Del Amo reports financial support was provided by Orion Research Fundation. Sina Bahrpeyma reports financial support was provided by Kuopio research foundation. Sina Bahrpeyma reports financial support was provided by Silmä- ja kudospankkisäätiö. Sina Bahrpeyma reports financial support was provided by Sokeain Ystävät.

Acknowledgement

Shirin Tavakoli and Arto Urtti acknowledge the research support from European Union's Horizon 2020 research and innovation program Marie Sklodowska-Curie Innovative Training Networks (ITN) Nanomed (grant no. 676137). Shirin Tavakoli also acknowledges Finnish Pharmaceutical Society and Sokeain Ystävät grant. Tatu Lajunen and Arto Urtti acknowledge support from Business Finland (#4208/31/2015). Tatu Lajunen received additional funding from Orion ResearchFoundation (#9-8214-9), Phospholipid Research Center (#TLA-2019-068/1-1), Instrumentarium Science Foundation and Silmäsäätiöiden Tohtoritutkijapooli and Eva del Amo from Orion Research Foundation and the strategic funding of the University of Eastern Finland. Sina Bahrpeyma and Jooseppi Puranen acknowledge Doctoral School of the University of Eastern Finland. Sina Bahrpeyma is grateful to Kuopio Research Foundation, Eye and Tissue Bank Foundation (Silmä- ja kudospankkisäätiö), and Sokeain Ystävät. We thank Timo Oksanen for his help in UPLC analysis. Ocular Drug Development Laboratory infrastructure, University of Eastern Finland is acknowledged for supporting the *in vivo* experiments.

Appendix A. Supplementary material

Supplementary data to this article can be found online at https://doi.org/10.1016/j.ijpharm.2022.121725.

References

Al-Khersan, H., Hussain, R.M., Ciulla, T.A., Dugel, P.U., 2019. Innovative therapies for neovascular age-related macular degeneration. Expert Opin. Pharmacother. 20, 1879–1891.

Campochiaro, P.A., 2013. Ocular neovascularization. J. Mol. Med. (Berl.) 91, 311–321.

Del Amo, E.M., Vellonen, K.S., Kidron, H., Urtti, A., 2015. Intravitreal clearance and volume of distribution of compounds in rabbits: In silico prediction and pharmacokinetic simulations for drug development. Eur. J. Pharm. Biopharm. 95, 215–226. https://doi.org/10.1016/j.ejpb.2015.01.003.

del Amo, E.M., Rimpelä, A.-K., Heikkinen, E., Kari, O.K., Ramsay, E., Lajunen, T., Schmitt, M., Pelkonen, L., Bhattacharya, M., Richardson, D., Subrizi, A., Turunen, T., Reinisalo, M., Itkonen, J., Toropainen, E., Casteleijn, M., Kidron, H., Antopolsky, M., Vellonen, K.-S., Ruponen, M., Urtti, A., 2017. Pharmacokinetic aspects of retinal drug delivery. Prog. Retin. Eye Res. 57, 134–185.

Ferrara, N., 2016. VEGF and Intraocular Neovascularization: From Discovery to Therapy. Sci. Tech. 5, 10. https://doi.org/10.1167/tvst.5.2.10.

Ferrara, N., Adamis, A.P.T., 2016. years of anti-vascular endothelial growth factor therapy. Nat. Rev. Drug Discov. 15, 385–403. https://doi.org/10.1038/nrd.2015.17.

Giddabasappa, A., Lalwani, K., Norberg, R., Gukasyan, H.J., Paterson, D., Schachar, R.A., Rittenhouse, K., Klamerus, K., Mosyak, L., Eswaraka, J., 2016. Axitinib inhibits retinal and choroidal neovascularization in in vitro and in vivo models. Exp. Eye Res. 145, 373–379. https://doi.org/10.1016/j.exer.2016.02.010.

Higuchi, T., Connors, K.A., 1965. Phase-solubility techniquese. Adv. Anal. Chem. Instrum. 4, 117–212.

Jager, R.D., Mieler, W.F., Miller, J.W., 2008. Age-Related Macular Degeneration. N. Engl. J. Med. 358, 2606–2617. https://doi.org/10.1056/NEJMra0801537.

Jain, A., Jain, S.K., 2016. In vitro release kinetics model fitting of liposomes: An insight. Chem. Phys. Lipids 201, 28–40. https://doi.org/10.1016/J.CHEMPHYSLIP.2016.10.005.

Janoria, K.G., Gunda, S., Boddu, S.H.S., Mitra, A.K., 2007. Novel approaches to retinal drug delivery. Expert Opin. Drug Deliv. 4, 371–388.

Kari, O.K., Tavakoli, S., Parkkila, P., Baan, S., Savolainen, R., Ruoslahti, T., Johansson, N.G., Ndika, J., Alenius, H., Viitala, T., Urtti, A., Lajunen, T., 2020. Light-Activated Liposomes Coated with Hyaluronic Acid as a Potential Drug Delivery System. Pharmaceutics 12 (8), 763.

Motzer, R.J., Rini, B.I., Bukowski, R.M., Curti, B.D., George, D.J., Hudes, G.R., Redman, B.G., Margolin, K.A., Merchan, J.R., Wilding, G., Ginsberg, M.S., Bacik, J., Kim, S.T., Baum, C.M., Michaelson, M.D., 2006. Sunitinib in patients with metastatic renal cell carcinoma. J. Am. Med. Assoc. 295 (21), 2516.

Nowak-Sliwinska, P., Weiss, A., van Beijnum, J.R., Wong, T.J., Kilarski, W.W., Szewczyk, G., Verheul, H.M.W., Sarna, T., van den Bergh, H., Griffioen, A.W., 2015. Photoactivation of lysosomally sequestered sunitinib after angiostatic treatment causes vascular occlusion and enhances tumor growth inhibition. Cell Death Dis. 6 (2), e1641.

Patel, J.K., Sutariya, V., Kanwar, J.R., Pathak, Y.V., 2018. Drug Delivery for the Retina and Posterior Segment Disease; Springer International Publishing. ISBN 9783319958071.

Peyman, G.A., Lad, E.M., Moshfeghi, D.M., 2009. Intravitreal injection of therapeutic agents. Retina 29, 875–912.

Ramazani, F., Hiemstra, C., Steendam, R., Kazazi-Hyseni, F., Van Nostrum, C.F., Storm, G., Kiessling, F., Lammers, T., Hennink, W.E., Kok, R.J., 2015. Sunitinib microspheres based on [PDLLA-PEG-PDLLA]-b-PLLA multi-block copolymers for ocular drug delivery. Eur. J. Pharm. Biopharm. 95, 368–377. https://doi.org/10.1016/j.ejpb.2015.02.011.

Robbie, S.J., Lundh von Leithner, P., Ju, M., Lange, C.A., King, A.G., Adamson, P., Lee, D., Sychterz, C., Coffey, P., Ng, Y.-S., Bainbridge, J.W., Shima, D.T., 2013. Assessing a novel depot delivery strategy for noninvasive administration of VEGF/PDGF RTK inhibitors for ocular neovascular disease. Investig. Ophthalmol. Vis. Sci. 54 (2), 1490.

Roskoski, R., 2007. Sunitinib: A VEGF and PDGF receptor protein kinase and angiogenesis inhibitor. Biochem. Biophys. Res. Commun. 356, 323–328.

Sakurai, Y., Ohgimoto, K., Kataoka, Y., Yoshida, N., Shibuya, M., 2005. Essential role of Flk-1 (VEGF receptor 2) tyrosine residue 1173 in vasculogenesis in mice. Proc. Natl. Acad. Sci. U. S. A. 102, 1076–1081. https://doi.org/10.1073/pnas.0404984102.

Schmitt, M., Hippeläinen, E., Raviña, M., Arango-Gonzalez, B., Antopolsky, M., Vellonen, K.-S., Airaksinen, A.J., Urtti, A., 2019. Intravitreal Pharmacokinetics in Mice: SPECT/CT Imaging and Scaling to Rabbits and Humans. Mole. Pharmac. 16 (10), 4399–4404.

Streets, J., Bhatt, P., Bhatia, D., Sutariya, V., 2020. Sunitinib-Loaded MPEG-PCL Micelles for the Treatment of Age-Related Macular Degeneration. Sci. Pharm. 88, 30. https://doi.org/10.3390/scipharm88030030.

Takahashi, H., Obata, R., Tamaki, Y., 2006. A novel vascular endothelial growth factor receptor 2 inhibitor, SU11248, suppresses choroidal neovascularization in vivo. J. Ocul. Pharmacol. Ther. 22, 213–218. https://doi.org/10.1089/jop.2006.22.213.

Tavakoli, S., Peynshaert, K., Lajunen, T., Devoldere, J., del Amo, E.M., Ruponen, M., De Smedt, S.C., Remaut, K., Urtti, A., 2020. Ocular barriers to retinal delivery of intravitreal liposomes: Impact of vitreoretinal interface. J. Control. Release 328, 952–961.

Tavakoli, S., Kari, O.K., Turunen, T., Lajunen, T., Schmitt, M., Lehtinen, J., Tasaka, F., Parkkila, P., Ndika, J., Viitala, T., Alenius, H., Urtti, A., Subrizi, A., 2021. Diffusion and Protein Corona Formation of Lipid-Based Nanoparticles in the Vitreous Humor: Profiling and Pharmacokinetic Considerations. Mol. Pharm. 18 (2), 699–713.

Tsujinaka, H., Fu, J., Shen, J., Yu, Y., Hafiz, Z., Kays, J., McKenzie, D., Cardona, D., Culp, D., Peterson, W., Gilger, B.C., Crean, C.S., Zhang, J.-Z., Kanan, Y., Yu, W., Cleland, J.L., Yang, M., Hanes, J., Campochiaro, P.A., 2020. Sustained treatment of retinal vascular diseases with self-aggregating sunitinib microparticles. Nat. Commun. 11 (1).

Urtti, A., 2006. Challenges and obstacles of ocular pharmacokinetics and drug delivery. Adv. Drug Deliv. Rev. 58, 1131–1135.

Varela-Fernández, R., Díaz-Tomé, V., Luaces-Rodríguez, A., Conde-Penedo, A., García-Otero, X., Luzardo-Álvarez, A., Fernández-Ferreiro, A., Otero-Espinar, F., 2020. Drug delivery to the posterior segment of the eye: Biopharmaceutic and pharmacokinetic considerations. Pharmaceutics 12 (3), 269.

Welsbie, D.S., Mitchell, K.L., Jaskula-Ranga, V., Sluch, V.M., Yang, Z., Kim, J., Buehler, E., Patel, A., Martin, S.E., Zhang, P.-W., Ge, Y., Duan, Y., Fuller, J., Kim, B.-J., Hamed, E., Chamling, X., Lei, L., Fraser, I.D.C., Ronai, Z.A., Berlinicke, C.A., Zack, D.J., 2017. Enhanced Functional Genomic Screening Identifies Novel Mediators of Dual Leucine Zipper Kinase-Dependent Injury Signaling in Neurons. Neuron 94 (6), 1142–1154.e6.

Welsbie, D.S., Ziogas, N.K., Xu, L., Kim, B.-J., Ge, Y., Patel, A.K., Ryu, J., Lehar, M., Alexandris, A.S., Stewart, N., Zack, D.J., Koliatsos, V.E., 2019. Targeted disruption of dual leucine zipper kinase and leucine zipper kinase promotes neuronal survival in a model of diffuse traumatic brain injury. Mol. Neurodegener. 14 (1) https://doi.org/10.1186/s13024-019-0345-1.

Wong, W.L., Su, X., Li, X., Cheung, C.M.G., Klein, R., Cheng, C.-Y., Wong, T.Y., 2014. Global prevalence of age-related macular degeneration and disease burden projection for 2020 and 2040: a systematic review and meta-analysis. The Lancet Global Health 2 (2), e106–e116.

World report on vision Available online: https://www.who.int/publications/i/item/world-report-on-vision (accessed on Nov 3, 2020).

Zhang, T., Xiang, C.D., Gale, D., Carreiro, S., Wu, E.Y., Zhang, E.Y., 2008. Drug transporter and cytochrome P450 mRNA expression in human ocular barriers: Implications for ocular drug disposition. Drug Metab. Dispos. 36, 1300–1307. https://doi.org/10.1124/dmd.108.021121.